DTU Library

Glare potential evaluation of structured PV glass based on gonioreflectometry

Babin, Markus; Thorsteinsson, Sune; Jakobsen, Michael Linde; Spataru, Sergiu Viorel

Published in:
IEEE Journal of Photovoltaics

Publication date:
2022

Document Version
Peer reviewed version

Citation (APA):
Babin, M., Thorsteinsson, S., Jakobsen, M. L., & Spataru, S. V. (2022). Glare potential evaluation of structured PV glass based on gonioreflectometry. *IEEE Journal of Photovoltaics*, *12*(6), 1314 - 1318.

Glare potential evaluation of structured PV glass based on gonioreflectometry

Markus Babin, *Graduate Student Member, IEEE*, Sune Thorsteinsson, Michael L. Jakobsen, Sergiu V. Spataru

***Abstract*—Potential glare through reflected sunlight can be a significant hindrance factor for PV installations, especially for building-integrated photovoltaics (BIPV) with atypical orientations and tilt angles present. Structured glass surfaces or anti-reflective (AR) coatings are often used as a solution, however there currently is no universally recognized method or metric for estimating their impact on glare.**

This work presents an evaluation of the glare potential of different surface glasses for use in PV modules based on their bi-directional reflectance distribution functions (BRDF). BRDF threshold values for retinal burn damage, flash blindness and discomfort glare are calculated based on retinal irradiance thresholds from literature. Subsequently, gonioreflectometric measurements on PV mini-modules are used to characterize the reflectance profiles of eight different glass surfaces.

Results for all measured structured glasses, both satinated and macro-textured, show significant reductions in BRDF compared to smooth glass, largely eliminating the potential for flash blindness as well as discomfort glare at low incidence angles. At high incidence angles, increased potential for discomfort glare as well as forward scattering along the glass surface can be observed. AR coatings, however, are shown to be insufficient to eliminate glare causing flash blindness.

***Index Terms*—Glare, Reflectometry, PV Module Materials, Encapsulation and Manufacturing, Characterization of PV**

I. Introduction

GLARE is a condition of high luminance or unsuitable luminance distribution that affects vision and can be separated into two categories: Discomfort glare is caused by a bright source within the field of view, compared to the surrounding, which may or may not impair vision. Disability glare, on the other hand, reduces vision, often caused by a reduced contrast of the entire field of view [1]. Beside affecting vision, very high levels of retinal irradiance can also cause permanent or temporary damage in the form of retinal burns or flash blindness.

Like all glazed surfaces, PV modules can cause glare, which presents a significant hindrance factor for PV installations, especially in urban settings and close to highways or airports. While there are no international standards regarding glare from PV installations, installations generating glare are prohibited in many national, local or regional building codes or other regulations, e.g. Federal Aviation Administration (FAA) guidelines. While (legal) assessment of glare mostly happens post construction on a case-by-case basis, large PV plants often employ simulation tools early in the planning phase to identify possible risks of glare. For small-scale installations, however, such simulations are rarely used, as their availability is limited and their cost can be notable. In any case, there is currently no universally recognized method or metric for the assessment of glare from PV [2], [3].

Conventional building-applied PV (BAPV) systems, i.e. mounted on roofs with low tilt angles, are unlikely to cause glaring reflections on ground level simply by virtue of their orientation and tilt. However, in building integrated PV (BIPV) systems, a wide variety of mounting configurations is used, ranging from semi-transparent skylights and PV windows to roof- or façade-integrated modules. With this plethora of options, however, also comes a risk of glare at various times of day and locations affected by it.

One common tool for simulating glare from PV installations was developed by Sandia National Laboratories under the name "Solar Glare Hazard Analysis Tool (SGHAT)" and is licensed out for third-party simulation tools, such as ForgeSolar [4]. It determines glare based on direct (specular) reflections from flat PV modules and determines the ocular impact.

Glare is mainly caused by specular reflections, i.e. reflections at view angles equal to the incidence angle of light. To reduce these reflections, and therefore the glare potential of PV products, manufacturers either use anti-reflective coatings or texturize the glass surface, e.g. through satination, which changes its reflective properties. Additionally, the reduced reflection losses from structured glass can lead to increased performance compared to flat PV glass, especially at high incidence angles, as has been shown through experimental measurements of incidence angle modifiers (IAM) [5].

Instead of characterizing the reflective properties of each individual glass surface, however, simulation tools often rely on generic reflectance profiles [4]. The SGHAT, for example, includes five reflectance fit functions: One each for smooth and lightly textured glass with and without an anti-reflective coating, and one for a deeply textured glass [6].

Due to the larger variety and complexity of glass treatments used in BIPV, the use of reflectance fit functions describing only specular reflections may be insufficient. Instead, the bi-directional reflectance distribution function (BRDF) can be used to fully describe the reflective properties of surfaces [7]. It describes the reflectance of a surface as a function of both incidence and view angle and can be measured using gonioreflectometers.

Before ray-tracing simulations are necessary, it should be

M. Babin, S. Thorsteinsson, M.L. Jakobsen and S.V. Spataru are with Department of Electrical and Photonics Engineering, Technical University of Denmark, Denmark.

Manuscript submitted May 30, 2022; revised June 29, 2022

possible to assess the overall glare-potential of a specific glass surface based only on its measured BRDF. This work attempts to lay the foundation for such an assessment as well as a comparison of the glare potential for different glass surfaces.

II. Theory & Methodology

A. Definition of glare levels

Whether or not glare causes damage to the eye depends on a variety of factors, mainly the radiance of the source, its distance and size, as well as the optical properties of the eye. For daylight conditions, good approximations exist for the human eye's pupil transmittance ($\tau \approx 0.5$), the pupil diameter ($d_p \approx 2\,\mathrm{mm}$) and focal length ($f \approx 17\,\mathrm{mm}$), which allows the determination of retinal irradiance E_r based on the radiance L_s emitted from a light source or reflective surface [8]:

$$E_r \approx \frac{\pi L_s \tau}{4}\left(\frac{d_p}{f}\right)^2 \approx \frac{\pi}{578} L_s \tag{1}$$

This radiance L_s describes the radiant power emitted from the surface in a certain direction α per solid angle and surface area and is given in $\mathrm{W/m^2/sr}$. The bi-directional reflectance distribution function (BRDF) correlates this radiance with the irradiance E_s received on the surface from direction θ:

$$B(\theta, \alpha) = \frac{dL_s(\alpha)}{dE_s(\theta)} \tag{2}$$

Since the BRDF is an angular dependent quantity, its unit is sr^{-1}, referring to the solid angle the light is reflected to. If we observe reflected light in the plane of incidence, as defined by the directions of the surface normal and incident light, the BRDF is reduced to a two-dimensional problem. Furthermore, the derivative can be dropped if only light from a single source is considered. Using this definition, the radiance L_s originating from a reflecting surface can be translated into the product of BRDF $B(\theta, \alpha)$, as a function of incidence angle θ and view angle α, and the solar irradiance E_s, resulting in the following equation for the retinal irradiance E_r:

$$E_r \approx \frac{\pi}{578} B(\theta, \alpha) E_s \tag{3}$$

According to comparative literature studies [8], limits for retinal burn damage range between approximately 100–$400\,\mathrm{kW/m^2}$ of retinal irradiance, and values for flash blindness range from 0.1–$1\,\mathrm{kW/m^2}$. Other studies [3] have reported similar radiance and/or irradiance threshold values for flash blindness. Assuming a typical angle of $9.3\,\mathrm{mrad}$ subtended by the sun and solar irradiance of $1\,\mathrm{kW/m^2}$, this results in an upper limit of $B(\theta, \alpha) < 18\,\mathrm{sr}^{-1}$ for the BRDF to avoid flash blindness.

Discomfort or disability glare may already start at significantly lower levels, which are dependent on a large number of factors influencing perception of glare as well as individual bias. Studies show average discomfort glare thresholds at 5.2–$4.7\log\mathrm{Td}$ (measured in Troland, a unit of retinal illuminance $E_{r,\nu}$), depending on the glare source size [9]. Approximations for unit conversions from $\log\mathrm{Td}$ to lx are shown in Equation 4 and for conversions from illuminance $E_{r,\nu}$ to irradiance E_r in Equation 5:

$$E_{r,\nu} = x[\log\mathrm{Td}] \approx \frac{10^x}{278}[\mathrm{lx}] \tag{4}$$

$$E_r \approx \frac{E_{r,\nu}}{120\,[\mathrm{W/(m^2lx)}]} \tag{5}$$

While values from these experiments may not be directly transferrable to glare from PV installations outdoors, using them as rough estimates results in glare occurring at irradiances as far down as 1.5–$4.8\,\mathrm{W/m^2}$. This in turn would result in BRDF limits of $B(\theta, \alpha) < 0.25$–$0.85\,\mathrm{sr}^{-1}$ to avoid glare altogether. An overview of all the glare threshold values are given in Table I.

B. BRDF measurements

For comparative BRDF measurements, eight single-cell mini-modules with different cover glasses are laminated using 2-busbar mono-crystalline Si cells, ethylene-vinyl acetate (EVA) as encapsulant and a black polymeric backsheet. Gonioreflectometric measurements are taken using the setup shown in Figure 1 which has been described in [10] and [11], with the reflective collimator elevated to the plane of irradiance in order to capture specular reflections.

Reflected light is measured in the spectral range between 300–$980\,\mathrm{nm}$ and related to the incident light to determine the BRDF. Measurements are taken in 15° steps of incidence angles θ between 0° and 75°, and at 5° steps of view angles α, constrained to between $-80°$ and $80°$. In the regions around specular reflection angles ($\theta = \alpha$), additional measurements in

TABLE I
Glare Threshold Values

Glare type	Retinal irradiance E_r [$\mathrm{kW/m^2}$]	BRDF [sr^{-1}]
Retinal burn damage	100–400	$(1.8–7.4) \times 10^4$
Flash blindness	0.1–1	18–184
Discomfort glare	1.5–4.8	0.25–0.85

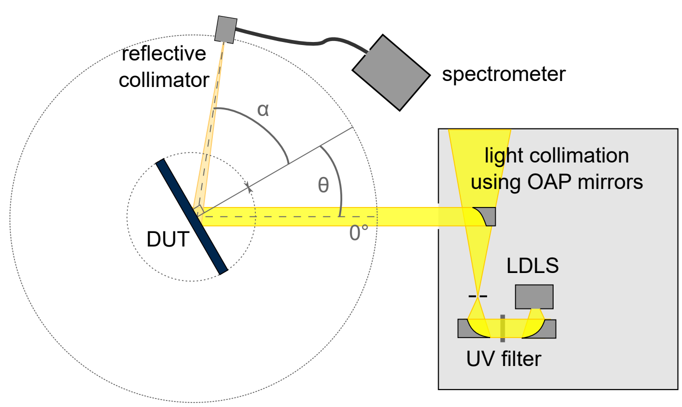

Fig. 1. Gonioreflectometer setup: Broadband light from a laser-driven light source (LDLS) is collimated by a set of off-axis parabolic (OAP) mirrors and UV light filtered out. The collimated light reflected from the device under test (DUT), mounted on a rotational stage, is gathered by an independently rotating reflective collimator and measured using a spectrometer.

0.5° steps are taken. For these measurements, neutral-density filters (2x Thorlabs NE10A) are placed between light source and the device under test (DUT) in order to avoid saturation of the spectrometer through specularly reflected light.

III. Measurement results

Figure 2a shows the single-plane BRDF of a PV mini-module with a reference PV glass. This tempered, low-iron float glass features a slight deviation from an even surface structure. This sample represents glass commonly used for PV modules.

Its BRDF profile shows distinctive peaks around specular reflection angles with a uniform spread indicating significant forward scattering of light on the glass surface. At higher incidence angles, the BRDF increases, especially for specular reflection angles, following an exponential relationship as shown (fitted empirically). There is relatively low Lambertian scattering, as signified by the baseline BRDF, which is almost constant over view angles but slightly reduced when specular reflections increase.

The measured BRDF of this reference glass surpasses the threshold for discomfort or disability glare at several angles close to specular reflection angles and at higher incidence angles even exceeds the limits for likely flash blindness. This is in good agreement with observations in real-world situations, where direct reflections from PV installations are slightly diffused, but can cause significant amounts of glare.

As comparison, Figure 2b shows the single-plane BRDF of a PV mini-module with a completely smooth glass surface. High reflectances are limited to specular reflection angles with close to no light diffusion through surface scattering. At the same time, BRDF values at specular reflection angles are significantly higher than those of the reference PV glass, surpassing the lower threshold for possible flash blindness at all measured incidence angles.

An identical glass with a single-layer anti-reflective coating has been used to laminate another sample, with its single-plane BRDF shown in Figure 2c. This coating leads to a significant reduction in BRDF compared to the smooth glass, especially at low incidence angles. At higher incidence angles this effect is less pronounced, possibly because the coating thickness is optimized to achieve destructive interference of reflected light at specific incidence angles. At higher incidence angles, this effect is still present but experiences a wavelength shift towards longer wavelengths and becomes less effective.

While there is a significant reduction in BRDF due to the AR coating, it nevertheless exceeds the threshold values for discomfort glare at all measured angles and can likely cause flash blindness at higher incidence angles. In this manner, it is similarly effective as the very slight surface structuring of the reference PV glass. In addition, the AR coating leads to a slightly higher degree of surface scattering, most likely due to its porous structure [12].

In BIPV, the common go-to solution to avoid glare is to choose a finely structured surface glass, commonly referred to as satinated. Figure 3 shows the single-plane BRDF of two PV mini-modules with satinated glass created by two different processes: sandblasting and acid-etching.

For Figure 3a, a reference PV glass was sandblasted, resulting in an irregular micro-textured surface that significantly increases surface scattering. Consequently, the BRDF profile shows significantly higher values at non-specular reflection angles, simultaneously there are no observable specular reflections at all. As a result, reflections only exceed the threshold for discomfort glare at high incidence angles. One notable feature, however, is the increased forward-scattering along the

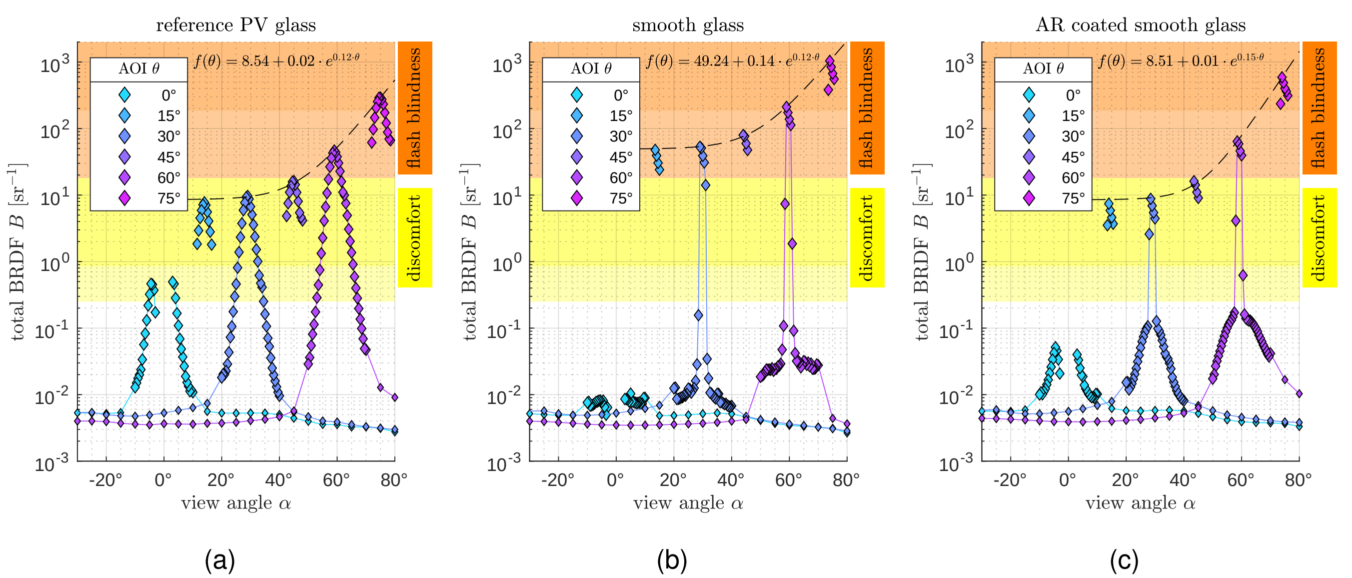

Fig. 2. Single-plane BRDF of samples with (a) reference PV glass (b) smooth glass (c) smooth glass with ARC. For incidence angles of 0°, 30° and 60°, data points for all measured view angles α are shown. For incidence angles of 15°, 45° and 75°, only data points around specular reflection angles are shown. Areas of potential discomfort/disability glare and flash blindness are highlighted through background colors. BRDF at specular reflection angles are fitted with an exponential function $B(\theta) = a + be^{c\theta}$.

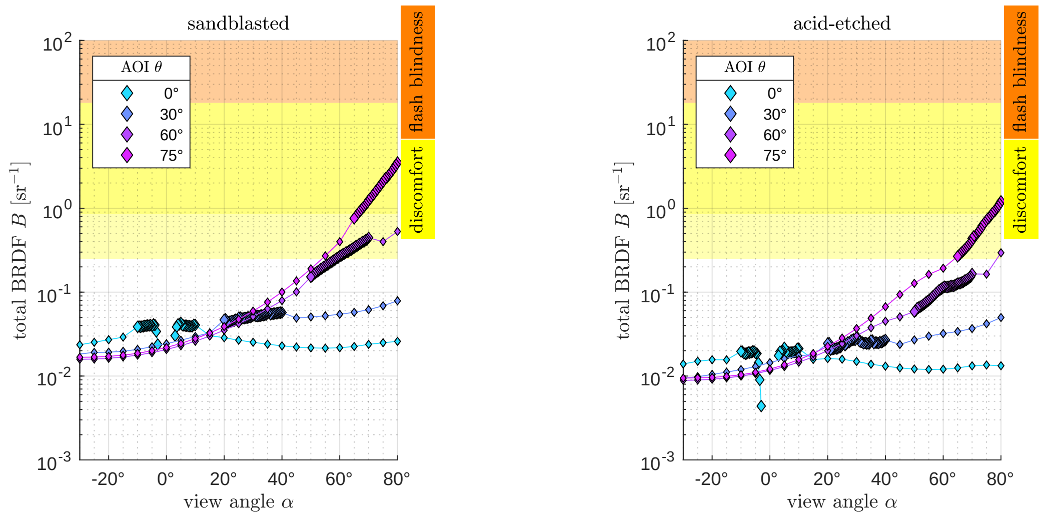

(a) (b)

Fig. 3. Single-plane BRDF of samples with (a) sandblasted PV glass (b) acid-etched glass for incidence angles of 0°, 30°, 60° and 75°.

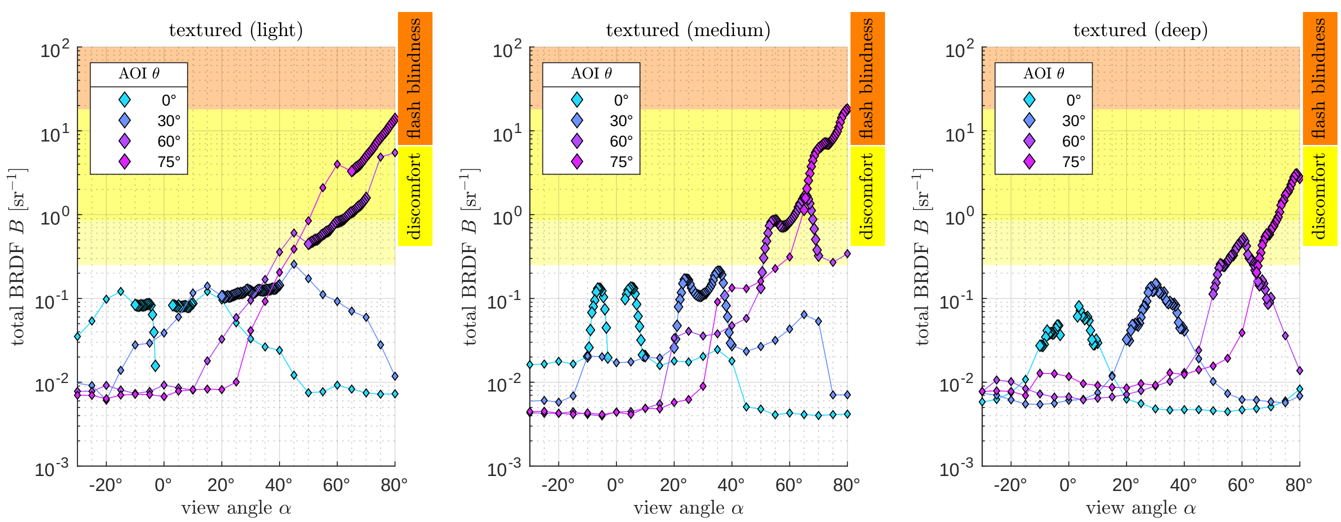

(a) (b) (c)

Fig. 4. Single-plane BRDF of samples with (a) lightly textured glass (b) medium textured glass (c) deeply textured glass with grooves. Data points are shown for incidence angles of 0°, 30°, 60° and 75°.

surface at high incidence angles which can reach values above those at specular reflection angles.

Similar observations can be made for the BRDF of PV modules with acid-etched surface glass, as shown in Figure 3b. This technology leads to overall slightly reduced reflections but otherwise identical observations.

The main alternative to satinated glass is the use of glass with an embedded texture. This macro-texture leads to a regular, uneven surface, often with pyramidal structures. Figure 4 shows the single-plane BRDF profiles of mini-modules with three different surface textures.

The sample in Figure 4a features ”Albarino S” from Saint-Gobain glass, a lightly textured glass with pyramidal structures. As can be seen from the measured BRDF, it leads to a significant reduction in reflectance, however at higher incidence angles BRDF values exceed the thresholds for discomfort glare. In this regard it is less effective than the satinated glasses shown in Figure 3. Furthermore, reflections experience a large degree of surface scattering, leading to BRDF values exceeding the discomfort glare threshold at a wide variety of view angles at high incidence angles.

Figure 4b shows the single-plane BRDF of a sample with larger-scale surface texture, leading to reflectance peaks around specular reflection angles similar to the ones in Figure 2a. At specular reflection angles themselves, however, reflectance is reduced, resulting in local minima in the BRDF.

The maxima of the BRDF are similar to that of the lightly textured glass, exceeding the threshold for discomfort glare at higher incidence angles. At these angles, the effect of increased forward scattering along the surface can also be observed.

Finally, the BRDF of a deeply structured glass is shown in Figure 4c, specifically "Albarino G" from Saint-Gobain glass, which features undulating grooves in a checkerboard pattern. For this glass sample type significantly reduced reflections can be observed, with the measured BRDF values only exceeding the discomfort glare threshold at high incidence angles. Compared to the other textured glasses, this structure is more effective at high angles and does not prominently feature increased forward scattering along the glass surface.

IV. Summary & Discussion

A comparison of the measured BRDF profiles show that both satination and macro-texturing of glass can lead to significant reductions in reflectance, sufficient to mostly eliminate the risk of flash blindness through glare from PV installations. The increased reflectance at high incidence angles, however, nevertheless results in a substantial risk for discomfort or disability glare.

Most of the investigated textured samples also show increased forward scattering along the glass surface at high incidence angles, indicating that a consideration of only specular reflections for glare assessment is insufficient. Additionally, differently textured glasses can lead to significantly different degrees of surface scattering, possibly leading to discomfort glare at view angle deviations of more than $10°$ from specular reflection angles.

The importance of the increased reflections at high incidence angles may be somewhat reduced, as in most configurations a combination of very high incidence and view angles already results in the sun being visible within the observers field of view. The presence of a secondary source through glare from PV will therefore be most likely less detrimental than if it is the only source of high intensity light.

Compared to surface texturing, AR coatings on their own are insufficient to reduce the reflectance of PV modules below the threshold for possible flash blindness at high incidence angles. In combination with surface texturing, AR coatings may however contribute positively towards glare reduction. It should also be noted that in this work the total BRDF between $300–980\,\mathrm{nm}$ is considered, which does not completely capture the spectral effects of AR coatings, which is usually optimized for wavelengths within the visible spectrum. Nevertheless, this does not alleviate the problematic reflections at high incidence angles, which lead to a significant spectral shift.

Overall it should be noted that none of the measured samples even remotely shows reflectances able to cause permanent damage to they eye in terms of retinal burn. Except for arrangements where reflections are focused on a single point, glare from PV can therefore be considered discomforting or temporarily debilitating, but not medically dangerous. Nevertheless, PV installations near busy roads, airports, etc should be sited and oriented in a manner to prevent frequent occurrence of glare and PV installers may consider wearing sunglasses to further alleviate the risk of flash blindness or discomfort.

V. Conclusion & Outlook

In this work, gonireflectometric measurements were used to compare different glass surfaces used in PV installations and estimates their glare impact based on calculations of the retinal irradiance. While reflectances from smooth glasses exceed thresholds for both discomfort or disability glare and flash blindness, textured glass surfaces (both micro- and macro-textured) reduce reflectances to discomfort levels. At low incidence angles, the reduction in reflectance is sufficient to avoid glare from PV altogether. Throughout this work, no reflectance values leading to dangerous levels of retinal irradiance which may cause permanent eye damage are observable.

The results also show that raytracing of only specular reflections may underestimate glare from PV modules with structured glass surfaces (especially macro-textured), as non-specular reflection angles ($\alpha \neq \theta$) can show higher reflectivity. This is especially true at high incidence angles, where increased forward-scattering along the glass surface can be observed. Simulation tools such as SGHAT may therefore underestimate the reflections at non-specular reflection angles while simultaneously overestimating them at specular reflection angles. This could lead to inaccurate conclusions regarding the frequency of glare and the locations where it may be observed from. To improve glare simulation models and tools, they should therefore be based on BRDF measurements rather than reference profiles in order to accurately consider the reflection properties of PV module surfaces. While this will increase the complexity of calculations, it will be required to predict glare from BIPV installations with complex textured glass surfaces.

Since only the total BRDF of samples was compared, the spectral effects of AR coatings have not been captured in this work. To properly assess their impact on glare potential, the BRDF should be weighted with the solar spectrum. Furthermore, no samples featuring a combination of surface texturing and AR coating were investigated, so no final conclusion can be drawn on their usefulness for reducing glare from PV modules.

Acknowledgments

The work presented in this paper was supported by the Danish Energy Technology Development and Demonstration Program (EUDP) under project contract UnitSun 64021-1079 which is gratefully acknowledged.

The authors would also like to thank Adrian A. Santamaria Lancia for his contributions to the gonioreflectometer setup.

References

[1] *E-ILV: International Lighting Vocabulary*, 2nd ed., International Commission of Illumination. [Online]. Available: https://cie.co.at/e-ilv

[2] K. A. Berger, S. Boddaert, M. D. Buono, A. Federova, F. Frontini, S. Inoue, H. Ishii, K. Kapsis, J.-T. Kim, P. Kovacs, M. Machado, N. M. Chivelet, A. Schneider, V. Shabunko, and H. R. Wilson, "Multifunctional characterisation of BIPV – proposed topics for future international standardisation activities," IEA, Tech. Rep., February 2020.

[3] R. Schregle, C. Renken, and S. Wittkopf, "Spatio-temporal visualisation of reflections from building integrated photovoltaics," *Buildings*, vol. 8, no. 8, August 2018.

[4] Forge solar help. [Online]. Available: https://www.forgesolar.com/help/

[5] M. W. Amdemeskel, G. A. dos Reis Benatto, N. Riedel, B. Iandolo, R. S. Davidsen, O. Hansen, P. B. Poulsen, S. Thorsteinsson, A. Thorseth, and C. Dam-Hansen, "Indoor measurement of angle resolved light absorption by antireflective glass in solar panels," in *Proc. 33rd EUPVSEC*, September 2017.

[6] C. K. Ho, C. A. Sims, J. Yellowhair, and E. Bush, *Solar glare hazard analysis tool (SGHAT) technical reference manual*, Sandia National Laboratories, March 2015.

[7] F. E. Nicodemus, "Directional reflectance and emissivity of an opaque surface," *Appl. Opt.*, vol. 4, pp. 767–775, July 1965.

[8] C. K. Ho, C. M. Ghanbari, and R. B. Diver, "Hazard analyses of glint and glare from concentrating solar power plants," in *SolarPaces 2009*, September 2009.

[9] G. Bargary, Y. Jia, and J. L. Barbur, "Mechanisms for discomfort glare in central vision," *Investig. Ophthalmol. Vis. Sci.*, vol. 56, no. 1, pp. 464–471, January 2015.

[10] M. Babin, "Experimental characterization of angular dependent color perception of colored PV samples in combination with IAM measurements targeting building integrated photovoltaic products," Master's thesis, Technical University of Denmark, July 2020.

[11] M. Babin, A. A. Santamaria Lancia, A. Thorseth, and S. Thorsteinsson, "Characterisation of angular dependent optical properties of different coloring technologies employed in BIPV products," in *Proc. 37th EUPVSEC*, September 2020.

[12] B. M. Freiburger, K. Isbilir, F. Lisco, G. Womack, J. M. Walls, and C. S. Thompson, "Durable high-performance water-based anti-reflective coating for pv module glass," in *7th IEEE World Conference on Photovoltaic Energy Conversion*, September 2018.